

AAAAAAA

by
FRANCESCO IOLI

A DISSERTATION PRESENTED TO
THE DEPARTMENT OF CIVIL AND ENVIRONMENTAL ENGINEERING

IN FULFILLMENT OF THE REQUIREMENTS
FOR THE DEGREE OF
DOCTOR OF PHILOSOPHY
IN GEOINFORMATICS

POLITECNICO DI MILANO
MILANO, ITALY
MAY 2024

THIS THESIS HAS BEEN APPROVED BY
PROF. LIVIO PINTO, ADVISOR

POLITECNICO DI MILANO
DEPARTMENT OF CIVIL AND ENVIRONMENTAL ENGINEERING
MILANO, ITALY

©2024 – FRANCESCO IOLI
ALL RIGHTS RESERVED.



POLITECNICO
MILANO 1863

AAAAAAA

ABSTRACT

Lorem ipsum dolor sit amet, consectetuer adipiscing elit. Morbi commodo, ipsum sed pharetra gravida, orci magna rhoncus neque, id pulvinar odio lorem non turpis. Nullam sit amet enim. Suspendisse id velit vitae ligula volutpat condimentum. Aliquam erat volutpat. Sed quis velit. Nulla facilisi. Nulla libero. Vivamus pharetra posuere sapien. Nam consectetuer. Sed aliquam, nunc eget euismod ullamcorper, lectus nunc ullamcorper orci, fermentum bibendum enim nibh eget ipsum. Donec porttitor ligula eu dolor. Maecenas vitae nulla consequat libero cursus venenatis. Nam magna enim, accumsan eu, blandit sed, blandit a, eros.

Quisque facilisis erat a duis. Nam malesuada ornare dolor. Cras gravida, diam sit amet rhoncus ornare, erat elit consectetuer erat, id egestas pede nibh eget odio. Proin tincidunt, velit vel porta elementum, magna diam molestie sapien, non aliquet massa pede eu diam. Aliquam iaculis. Fusce et ipsum et nulla tristique facilisis. Donec eget sem sit amet ligula viverra gravida. Etiam vehicula urna vel turpis. Suspendisse sagittis ante a urna. Morbi a est quis orci consequat rutrum. Nullam egestas feugiat felis. Integer adipiscing semper ligula. Nunc molestie, nisl sit amet cursus convallis, sapien lectus pretium metus, vitae pretium enim wisi id lectus. Donec vestibulum. Etiam vel nibh. Nulla facilisi. Mauris pharetra. Donec augue. Fusce ultrices, neque id dignissim ultrices, tellus mauris dictum elit, vel lacinia enim metus eu nunc.

Contents

Listing of figures

Acknowledgments

LOREM IPSUM DOLOR SIT AMET, consectetur adipiscing elit. Morbi commodo, ipsum sed pharetra gravida, orci magna rhoncus neque, id pulvinar odio lorem non turpis. Nullam sit amet enim. Suspendisse id velit vitae ligula volutpat condimentum. Aliquam erat volutpat. Sed quis velit. Nulla facilisi. Nulla libero. Vivamus pharetra posuere sapien. Nam consectetur. Sed aliquam, nunc eget euismod ullamcorper, lectus nunc ullamcorper orci, fermentum bibendum enim nibh eget ipsum. Donec porttitor ligula eu dolor. Maecenas vitae nulla consequat libero cursus venenatis. Nam magna enim, accumsan eu, blandit sed, blandit a, eros.

1

Introduction

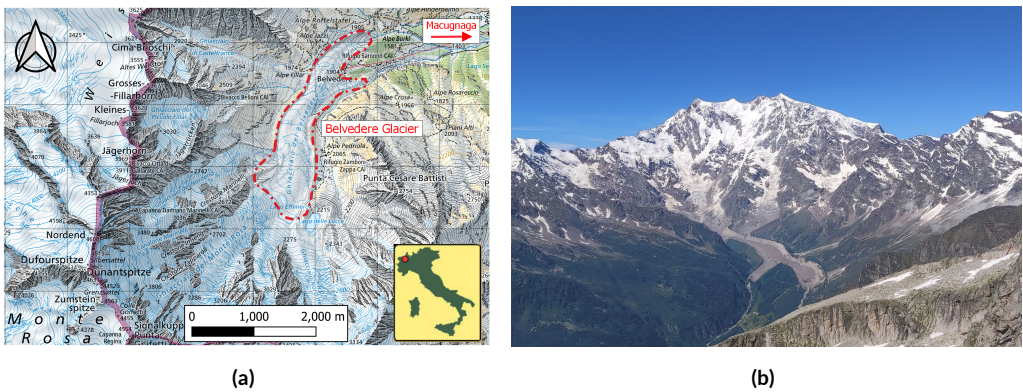


Figure 1.1: (a) Location of Belvedere Glacier, base map (source: Swisstopo www.geo.admin.ch); (b) Picture of ...

1.1 MOTIVATION AND RELEVANCE

1.2 THE BELVEDERE GLACIER

The Belvedere Glacier (Randolph Glacier Inventory code RGI60-11.02858) is an alpine glacier in Valle Anzasca (Italy), on the east side of the Monte Rosa Massif ($N\ 45^{\circ}58' E\ 7^{\circ}55'$) (Fig. ??). The lower part of the Belvedere Glacier is a temperate debris-covered glacier, that covers an area of $\sim 1.8\ km^2$ and extends from an altitude of $\sim 2250\ m\ a.s.l.$ to $\sim 1800\ m\ a.s.l.$. This region is characterized by a gentle slope, and it is fed by ice falls and snow avalanches coming from the Monte Rosa East Face (?). In its low-relief sector, the Belvedere Glacier splits into two lobes, reaching $\sim 1800\ m\ a.s.l.$. The northern lobe, in particular, ends with a prominent ice cliff, from which the River Anza springs.

Similarly to Miage glacier (Monte Bianco, Valle d'Aosta), the Belvedere Glacier is almost completely covered by rocks and boulders with dimensions ranging from few decimetres to some meters, which makes it a *black glacier*. Due to the global warming trend, the number of black glaciers along the Italian Alps is rising (?). Up to the beginning of the century, the debris cover helped to compensate the effect of the increased temperature, establishing a negative feedback in the temperature-ablation relationship (??). However, in recent years, the debris cover protection has not been sufficient to limit the glacier retreat.

In the past, several hazardous events originated by the Belvedere Glacier, such as floods and slope instability, threatened the nearby village of Macugnaga and the Zamboni Zappa Hut, at $2070\ m\ a.s.l.$ (?). At the beginning of the 21st century, the Belvedere Glacier was characterized by a particular surge-type dynamics (?). During the late 1990s, the surface speeds of the whole glacier were ranging between $30\ m\ y^{-1}$ and $45\ m\ y^{-1}$ (??). During 2000–2001 an accelerated flow in the Monte-Rosa Glacier produced a wave of compression-decompression

stresses and strains in the Belvedere Glacier. Surface velocities soared: values up to 200 m y^{-1} were observed photogrammetrically during autumn 2001 (?). The ice thickness increased more than 20 m and the wave travelled downwards, creating a depression area in the accumulation zone, that was filled by a super-glacial lake, the Lago Effimero (??).

2

Back to the past: reconstructing glacier geometry with historical aerial images (1977-2009)

THIS CHAPTER IS BASED ON:

De Gaetani, C. I., Ioli, F., & Pinto, L. (2021). Aerial and UAV Images for Photogrammetric Analysis of Belvedere Glacier Evolution in the Period 1977–2019. *Remote Sensing*, 13(18), 3787. <https://doi.org/10.3390/rs13183787>

2.1 INTRODUCTION

2.2 DATASETS

2.2.1 HISTORICAL AERIAL DATASETS OF 1977, 1991 AND 2001

2.2.2 DIGITAL AERIAL AND UAV DATASETS OF 2009 AND 2019

2.2.3 GNSS SURVEY FOR BLOCK GEOREFERENCING

2.3 METHODS

2.4 DISCUSSION

3

UAV photogrammetry for annual glacier reconstruction (2015-2023)

THIS CHAPTER IS BASED ON:

Ioli, F., Bianchi, A., Cina, A., De Michele, C., Maschio, P., Passoni, D., & Pinto, L. (2021). Mid-Term Monitoring of Glacier's Variations with UAVs: The Example of the Belvedere Glacier. *Remote Sensing*, 14(1), 28.
<https://doi.org/10.3390/rs14010028>

3.1 INTRODUCTION

4

Deep learning low-cost photogrammetry for 4D short-term glacier monitoring (2022-2023)

THIS CHAPTER IS BASED ON:

- Paper under review on PFG
- Ioli, F., Bruno, E., Calzolari, D., Galbiati, M., Mannocchi, A., Manzoni, P., Martini, M., Bianchi, A., Cina, A., De Michele, C., and Pinto, L. (2023). A REPLICABLE OPEN-SOURCE MULTI-CAMERA SYSTEM FOR LOW-COST 4D GLACIER MONITORING, Int. Arch. Photogramm. Remote Sens. Spatial Inf. Sci., XLVIII-M-1-2023, 137-144,
<https://doi.org/10.5194/isprs-archives-XLVIII-M-1-2023-137-2023>

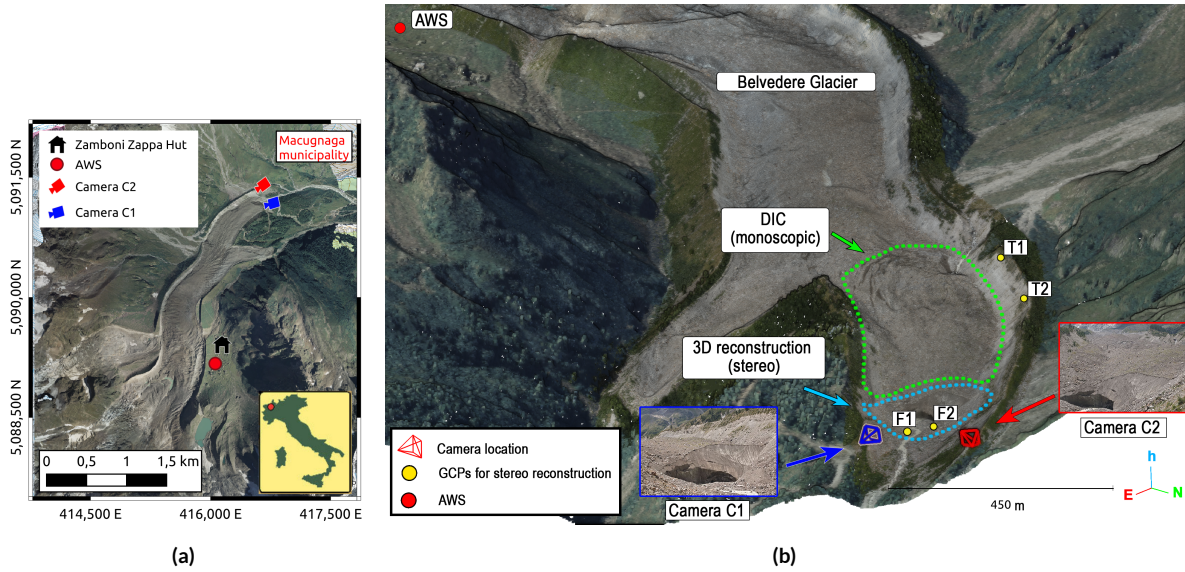


Figure 4.1: (a) Map of the Belvedere Glacier, with marked the location of the two cameras C1 and C2, the Automatic Weather Station (AWS) and the Zamboni Zappa Hut; (b) The area of study: the stereoscopic reconstruction is focused on the terminal ice cliff (dashed light blue line), while the monoscopic DIC processing from camera C2 image sequence is focused on the upper area of the north lobe (dashed green line).

4.1 INTRODUCTION

TODO: write introduction

4.2 THE LOW-COST STEREOSCOPIC SYSTEM

The low-cost stereoscopic system consists of two autonomous and independent monitoring units. Each unit is includes an off-the-shelf DSLR camera (Canon Eos 1200D), an Arduino microcontroller for camera triggering, and a Raspberry Pi Zero with a SIM card for sending images to a remote server via a GSM network(?). The instruments are housed in waterproof cases and mounted on tripods anchored to stable rocks along the glacier moraines. Power is supplied by a solar panel combined with a sealed lead-acid battery. The total cost of each unit was less than €2000, including camera and lens (?). The low-cost camera system is described in detail in ?.

The two monitoring stations, labelled as C₁ and C₂, were installed in summer 2021 on either side of the north tongue of Belvedere Glacier (Fig. ??). The harsh glacier environment with steep and unstable moraines, often subject to rockfall due to glacier retreat, constrained the camera installation location at ~230 m (camera C₁) and ~350 m (camera C₂) from the terminal ice cliff, with a strongly convergent pose. Different lenses

Table 4.1: Summary of the characteristics of the two cameras. Fields marked with * are computed considering the distance between each camera and the ice cliff.

	C ₁	C ₂
Camera	Canon Eos 1200D	Canon Eos 1200D
Sensor	APS-C	APS-C
Pixel size	3.7 μ m	3.7 μ m
Image	6000 \times 4000 px	6000 \times 4000 px
Lens	Canon EF 24mm f/2.8 IS USM	Canon EF 35mm f/2 IS USM
Distance*	230 m	350 m
Average GSD*	3.5 cm px ⁻¹	3.5 cm px ⁻¹

were used for the two cameras to achieve the same image scale in correspondence of the glacier tongue: C₁ was equipped with a 24 mm lens, while a 35 mm lens was used for C₂.

The baseline between the two cameras of \sim 261 m ensured a good viewing geometry because of the large parallax between corresponding points. However, the baseline comparable to the camera-object distance (base-height ratio close to 1, Tab. ??) led to complex affinity-like distortions and occlusions between corresponding areas in the two images (?). Additionally, C₁ was positioned at a lower viewpoint compared to C₂, due to site geometry constraints. Therefore, camera C₁ provides a limited view that primarily encompasses the frontal ice cliff, but does not capture the glacier surface, which is only visible from camera C₂.

The stereoscopic system was operating from August 2021 up to December 2022, when it was temporarily unmounted for ordinary maintenance, and finally mounted again in June 2023. During the operational period, the system was programmed to acquire two images per day, but only one image per day was used for the multitemporal processing. Only daily images taken during the snow-free period between 01/05/2022 and 13/11/2022 were considered. In this period, the glacier is experiencing the most significant changes, flow velocity and ablation rates. On the other hand, during winter and spring seasons, the glacier was covered by snow, making it difficult to extract relevant information from optical images for tasks such as 3D reconstruction and surface velocity estimation.

The low-cost stereoscopic system for continuous monitoring is composed of two independent units, each housing an off-the-shelves DSLR camera. Each unit consists in an autonomous monitoring station that provides power supply, internet connectivity, timing and scheduling of image acquisition, and protection from the harsh environment. The station was designed and built adapting to the alpine environment an existing open-source model developed by Greig Sheridan and published on GitHub¹. A key aspect of the project was

¹Greig Sheridan' Intervalometer repository: <https://github.com/greiginsydney/Intervalometer>

to ensure easy assembly and realization of the system to guarantee future replication or improvement by non-experts. In the following, we describe in detail the services and the nominal performances provided by our system that make it worth consideration for applications in different monitoring contexts. Refer to Fig. ?? for a descriptive schematic of the whole system showing the components selected for the Belvedere Glacier case study. The choice of the camera and optics is discussed in Section XX, as these components are dependent on the domain of use of the stereoscopic system.

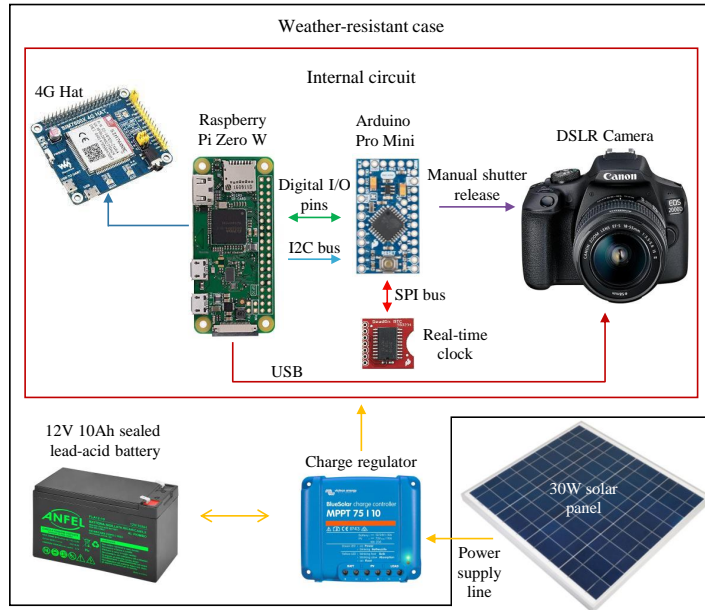


Figure 4.2: Scheme of the proposed acquisition system configuration for a single monitoring station. Arrows indicate the direction of signal initiation. Image adapted from Greig Sheridan's repository.

4.2.1 POWER SUPPLY

Each monitoring unit has its autonomous power supply line (yellow arrows in Figure ??) provided by a solar panel combined with a sealed lead-acid battery. An MPPT (Maximum Power Point Tracker) charge regulator directly connects with the unit's internal circuit, providing a regular current supply to the battery and the load and exploiting all the power generated by the panel. This regulator prevents any excess current that may damage the connected device, thus increasing the reliability of the system. Its battery life-saving algorithm modulates the load disconnection level so that a nearly 100% recharge is achieved about once every week and, in case of battery discharging, the whole system is switched off until 100% recharge of the battery is achieved. The whole

monitoring system is designed to minimise power consumption, e.g., by powering off devices responsible for the highest power consumption when not needed. An estimation of the system's energy consumption guided the choice of the components of the power supply line. Specifically, the battery and the associated panel must be accurately dimensioned for the system's purpose. To this end, the Photovoltaic Geographical Information System (PVGIS) (?), a tool provided by the European Commission, was used. PVGIS can estimate the performance of off-grid photovoltaic systems according to the installation site and it is supported by a database and algorithms for calculating solar radiation. Tuning the parameters for the Belvedere Glacier location and the system consumption, we ended up with the specifications of solar panel power of 30 W and battery voltage of 12 V and capacity of 10 Ah. Some compromises were made, accepting that the system would not be sufficiently powered in the months with lowest solar radiation (November, December, January, and February). [further details on PVGIS simulations for the Belvedere Glacier case study](#) re given.

4.2.2 SYSTEM CONTROL AND SCHEDULING

The internal electronic circuit (red box in Fig. ??) of the monitoring unit is the only load connected to the power supply and is responsible for all the system's control and scheduling functionalities. Its components are a real-time clock (number 3 in Fig. ??) with a 12 mm coin-cell backup battery, an Arduino microcontroller (Pro Mini 328 3.3V 8MHz, number 4 in Fig. ??), a Raspberry Pi Zero W with 128 GB SD memory card (number 6 in Fig. ??), and minor elements for connections, isolation (capacitors and optoisolators numbers 1 and 5 in Fig. ??), and voltage regulations (numbers 2 in Fig. ??). The circuit was realized manually by soldering wires and components on a stripboard (see Fig. ??).

The Arduino communicates through an SPI (Serial Peripheral Interface) bus with an accurate real-time clock to schedule its actions: waking the camera, firing the shutter to take a photo, and turning on/off the Raspberry. The Raspberry is able to access the camera images and transfer them to a remote server via internet connectivity. A large storage memory is added to the unit to save photos before remote transferring. The Raspberry also provides a web-based, user-friendly interface (Fig. ??) to configure and monitor the system remotely (?). An I₂C (Inter Integrated Circuit) bus and digital pin connections enable higher-level communication between these two boards. Among the minor components, we mention the role of the three voltage regulators. They allow each unit to be powered at the appropriate voltage and current: starting from the 12 V in input, one delivers 3.3 V and 500 mA to the Arduino, one 5 V and 2.5 A to the Raspberry and its hat, and the other 7.5 V and 2.4 A to the camera. The Arduino controls the 5V regulator of the Raspberry to reduce quiescent power consumption when the Raspberry board is off.

Acquisition of a defined number of images, camera triggering and timing, and sending of images to a

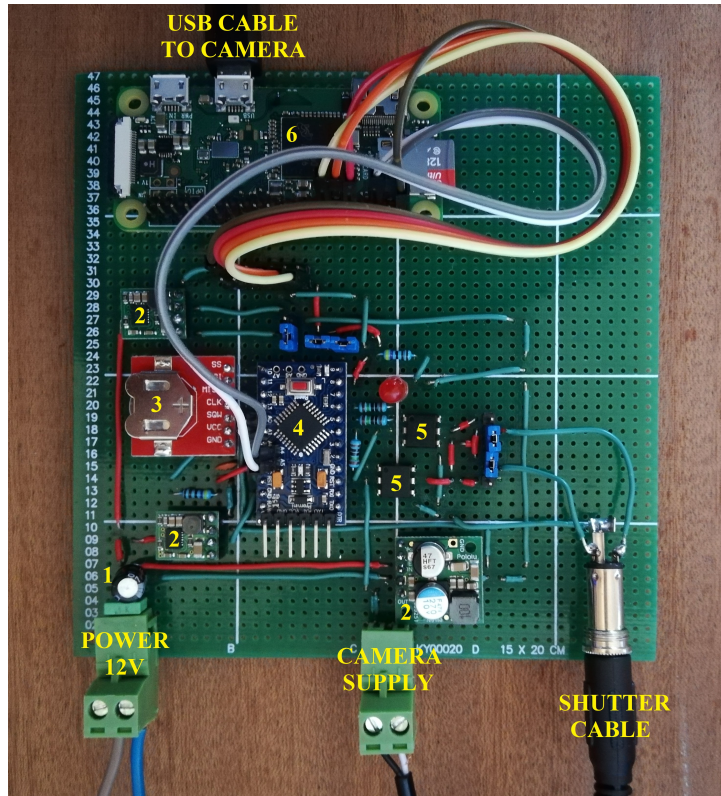


Figure 4.3: Stripboard on which are soldered the main components of the internal circuit: capacitors (1), voltage regulators (2), real-time clock with coin-cell battery (3), Arduino Pro Mini (4), optoisolators (5), and Raspberry Pi Zero W (6). [Add pic of new board](#)

remote server can be scheduled thanks to adequate programming of a cyclic executive program in C++ for Arduino and of services executing automatically Python scripts for the Raspberry. All the monitoring station activities can be remotely scheduled from the terminal or a user-friendly web interface (?). This useful feature allows one to change the settings and check the behaviour of the system, avoiding the need for manual intervention. The Raspberry uses the gPhoto2, a Python-based protocol developed to specifically interact with popular cameras' firmware, to communicate with the camera and access the new photos. The web-based interface service is based on NGINX and Gunicorn, open-source software for web servers. The interface (Fig. ??) consists of a web page accessible with credentials and provides a summary of the system state and the exact time of the last operations (time of the last shot and the last upload of images), temperatures of the components, previews of the last images, buttons to wake up the camera, take a preview photo and schedule the system routine (time and number of photo acquisition, wake-up time of the Raspberry) and some camera settings.

All the components were chosen because of their low power consumption and their inter-compatibility.

System Information	
System date:	2020 Sep 26 14:21:46
Last shot:	Saturday 14:00
Next shot:	Saturday 14:30
Camera:	USB PTP Class Camera
Lens:	EF24mm f/2.8
Images on camera:	1303
Last image on camera:	2020-09-26 14:02:48
Available shots:	127098
Battery:	100%
Images on Pi:	1286
Last image on Pi:	2020-09-25 18:32:48
Pi storage free:	100.07 GB
Last transfer:	2020/09/26 14:02:27 Commencing upload using Google Drive

Intervalometer Settings	
Shoot day of week:	Monday Tuesday Wednesday Thursday
Daily start hour:	07
Daily end hour:	20
Interval (minutes):	30
Shots / day:	26
Est days in camera:	Unknown
<input type="button" value="Apply"/>	

Thermal	
Units:	<input checked="" type="radio"/> °C <input type="radio"/> °F
Arduino temperature:	17 °C
Arduino min:	<input type="button" value="Reset"/> 8 °C
Arduino max:	<input type="button" value="Reset"/> 46 °C
Pi temperature:	37 °C

Figure 4.4: Example of some of the pages of the web-based interface to remotely control the monitoring units.

The circuit is robust against power losses due to battery discharging and is able to auto-recover when power is regained. A low energy consumption policy is also followed in selecting the scheduling. The camera is switched on only during the data capture activity. The Raspberry is switched on only once per day when the connection with the remote server and image transfer is scheduled.

4.2.3 CONNECTIVITY

Internet connectivity is crucial to transfer images and to control the units remotely. To this end, the Raspberry is equipped with the SIM7600E-H 4G hat by Waveshare. The module supports 4G/3G/2G communication via a SIM card. Raspberry and hat operations are the most expensive in terms of power consumption. For this reason, the board is switched on only once a day for a limited period of time, which is kept adequately low to be sustainable for the system power supply but still sufficient for transferring new images to the server. We adopted IoT (Internet of Things) SIM cards provided by the multi-operator service Emnify (?), as it offers the ability to connect to the best-quality cellular network available and includes flexible and customizable data plans. Remote access to the devices is allowed by a VPN (Virtual Private Network). The service costs €33 per month for a data plan with 6 GB.

4.2.4 CASE AND PROTECTION

The majority of the components need to be protected. Therefore, a solid and compact case that allows keeping all the parts (with the exception of the solar panel) in the same location is desirable for the functioning of the system and for convenient transportation, installation and maintenance. The case should also satisfy the thermal insulation requirements according to each component's working temperature range. The case should also be waterproof and robust against different and harsh weather conditions but, at the same time, provide access for connecting the solar panel and taking pictures. Our choice was an HPRC 2250 lightweight, waterproof resin case with internal insulating foam. The foam was found to be useful in enhancing the temperature seal and stabilising the location of some components, preventing unwanted movements. Holes were drilled in the case: one sealed with a UV filter of 82 mm to allow the camera to take shots, two others to give access to the solar panel wires, and others to fix the system to a tripod. The internal case dimensions (236x182x155 mm) posed a significant challenge in accommodating all the components inside. In particular, the camera lens dimensions were constrained by space availability.

4.2.5 GENERAL PERFORMANCES

The system was subject to several tests before being used in its final application at the Belvedere glacier site. During these tests, the system proved to be autonomous, robust to sudden shutdowns, cold-resistant, water-resistant and self-sufficient for a prolonged period of time with no direct sunlight on the solar panels. Specifically, in the absence of sunlight, the battery is able to power the system for about nine days before it is completely discharged. Battery voltage and temperatures of components were monitored, simulating the absence of solar radiation and low environmental temperatures. See Figure ?? for the performances of the system during these tests.

4.2.6 CAMERA AND LENSES

The choice of the DSLR camera and of the optics can be considered application-dependent. Therefore specifications regarding these components are reported in reference to the Belvedere glacier case study. Each monitoring station was equipped with a DSLR camera Canon EOS 2000D, with 24.1 MP CMOS APS-C sensor. This model was chosen because of the limited costs, the high image resolution and its compactness, as it must fit inside the case. Additionally, another fundamental requirement was camera compatibility with the gPhoto2 software. In the installation inside the system case, the traditional rechargeable battery was replaced by a special battery ("fake battery") equipped with a power supply cable, which provides a voltage of 7.5 V from the

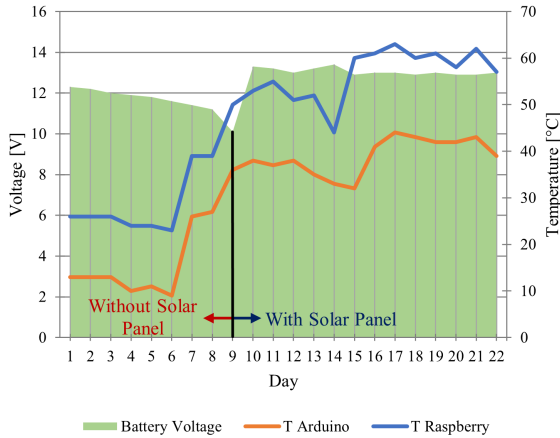


Figure 4.5: Battery voltage and temperature of boards with and without the solar panel during a period of tests. Starting from a fully charged condition, the system was kept without solar panel at around 2 °C for the first six days. After nine days, the battery was fully discharged and the system was reconnected to the panel and exposed to solar radiation.

circuit. The camera is attached to a sliding plate able to vary, with a limited range, and then fix the position of the camera on the longitudinal axis. Screws fix the camera to the plate and the plate to the case.

The two stations were installed respectively at ~ 180 m and ~ 340 m distance to the glacier terminus (see Fig. ??), avoiding the steep moraines of the glacier, often prone to collapses and landslides. Therefore, a wide baseline of ~ 260 m occurs between the two sensors. The final positioning of the two cameras was decisive in the choice of optics. In fact, to ensure comparable Ground Sample Distance (GSD) of the images ($\sim 3 \text{ cm px}^{-1}$), lenses with different focal lengths were employed. In particular, a Canon EF 24 mm f/2.8 IS USM and a Canon EF 35 mm f/2 IS USM were used respectively for Camera 1 (stream-wise right) and Camera 2 (stream-wise left).

4.2.7 CAMERA INSTALLATION

Monumentation of the two cameras at the Belvedere Glacier site was achieved by choosing two large stable rocks along the moraines. Each camera is supported by an aluminium topographic tripod system anchored with steel dowels and cables to the rocks (Fig. ??b). A central steel tie rod keeps the system in a fixed position. The choice of an agile monumentation was aimed at having a system that can be rather easily assembled on site (and also disassembled, if needed), also in a harsh environment, with limited costs and time. To install the cameras, in fact, all the equipment was carried in backpacks along the moraines, sometimes without a marked walking path (e.g., in the case of the stream-wise left camera). As a drawback, the analysis of the acquired photos revealed a non-optimal stabilization of the two cameras. In fact, small rotations, especially around the vertical axis, and

vibrations, mostly induced by the wind, were experienced. Though, a perfectly stable monummentation in a mountain environment is hardly achievable. Therefore, it is not possible to assume the camera orientation as stable a priori, but camera orientation must be estimated based on some Ground Control Points (GCPs) located on the ground in stable areas.

It is worth mentioning the performances of the system in terms of costs: our monitoring system can be fully reproduced with an average cost of €2000 per station (November 2023), including camera (€400), lens (€500) and material for the on-site installation (€150). In comparison, commercial time-lapse cameras are expensive (e.g., PhotoSentinel² cameras cost more than \$5,000.00) and hardly customizable. The final prototype of the monitoring station is shown in Figure ??.



Figure 4.6: (a) Picture of the monitoring unit prototype installed for tests at the Belvedere Glacier site. (b) Picture of the final monummentation of the camera installed on the stream-wise right moraine. **TODO: change picture with the final installation**

²PhotoSentinel: <https://photosentinel.com/> (accessed on 15/11/23)

4.3 DATASETS

4.3.1 STEREOSCOPIC IMAGE SEQUENCES

During the snow-free study period (from 1/05/2022 to 13/11/2022), both camera C₁ and camera C₂ were able to acquire images every day, for a total of 197 images. However, 39 images were discarded due to bad weather conditions, such as rain, low clouds, or fog, resulting in 158 days with valid data for stereo and monoscopic processing.

TODO: write about the images sequence 2022 and 2023

4.3.2 UAV SURVEYS

Two UAV flights, spaced by a 10-days interval, were conducted in summer 2022 to acquire ground truth data for assessing the proposed methodology. The first UAV flight, labelled as UAV-A, was carried out on 28/07/2022 with a DJI Matrice 300 RTK quadcopter and a DJI Zenmuse P1 camera with a 35 mm lens. During the survey, 436 images were captured, encompassing both nadiral and oblique perspectives. Additionally, 19 Ground Control Points (GCPs) were measured using a combination of a total station and Differential GPS (DGPS), employing a topographic-grade GNSS receiver. The GCPs included both artificial targets and natural features. During the flight, the UAV was equipped with an on-board RTK GNSS receiver, enabling the acquisition of camera projection centers with decimetric accuracy. The photogrammetric block (Fig. ??a) was processed with the commercial software package Agisoft Metashape (?) by using 14 GCPs and 5 Check Points (CPs) to evaluate the block accuracy. The global RMSE evaluated on the CPs was equal to 4.0 cm.

The second UAV flight, UAV-B, was carried out on 05/08/2022 with a DJI Phantom 4 RTK, focusing on a smaller portion of the northern lobe of the Belvedere Glacier. However, due to technical constraints, *moving* GCPs located inside the glacier body were not measured again. Therefore, only the fixed targets located outside the glacier were employed. Among these, 8 targets were designated as GCPs, while the remaining 4 were used as CPs. The photogrammetric block encompassed 428 nadiral and oblique images, which were processed using Agisoft Metashape (Fig. ??b). A global RMSE of 7.5 cm was obtained on the 4 CPs.

4.3.3 METEOROLOGICAL MONITORING STATION

To analyze the correlation between the Belvedere Glacier dynamics and external environmental variables, data measured from an Automatic Weather Station (AWS) located close to the Zamboni Zappa Hut were used. The AWS is located at an altitude of 2075 m a.s.l. and at a distance of 2 km from the area of study. In our study,

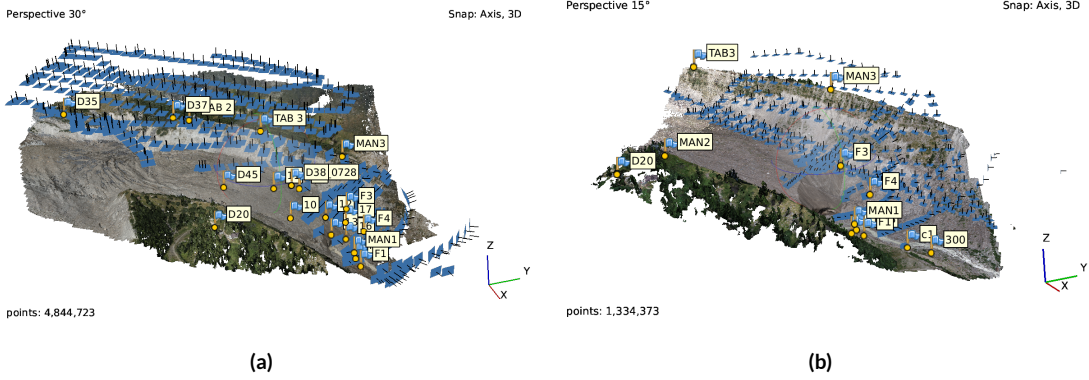


Figure 4.7: (a) UAV-A block and (b) UAV-B block processed with Agisoft Metashape. The flags represent the targets used either as GCPs in the BA or as CPs to evaluate the quality of the photogrammetric block.

we analyzed mean daily values of air temperature, precipitation and incoming solar radiation from 01/05/22 to 15/11/22.

4.4 METHODOLOGY

This chapter outlines the methodology developed to monitor the evolution of the Belvedere Glacier northern lobe. The daily images were processed using a framework consisting of two parallel processing chains (Fig. ??): (i) a photogrammetric-based stereoscopic approach; (ii) a DIC-based monoscopic approach. The daily stereo pairs were used to generate 3D models of the glacier terminus, enabling the estimation of ice volume loss on a daily basis by computing point cloud differences along the main flow direction. However, due to limited overlapping views of the two cameras, the stereoscopic approach primarily provides a 3D reconstruction of the terminal ice cliff (dashed-blue area in Fig. ??b). Consequently, deriving the 3D surface velocity field of the glacier solely from photogrammetry was not feasible. The image sequence captured by camera C₂, offering a higher viewpoint and broader coverage of the glacier surface, was employed to determine the glacier's surface velocity over a larger area of the north lobe of the Belvedere Glacier (dashed-green area in Fig. ??b).

4.4.1 IMAGE SELECTION

Once the acquired images have been received from the monitoring system, an automatic selection of the images was performed to exclude the ones acquired in rainy, foggy, or poor lighting conditions. This selection was based on the analysis of images median entropy (?): the images with a low value over the entire image were rejected. Additionally, a visual inspection was performed on the entire image dataset. The inspection had

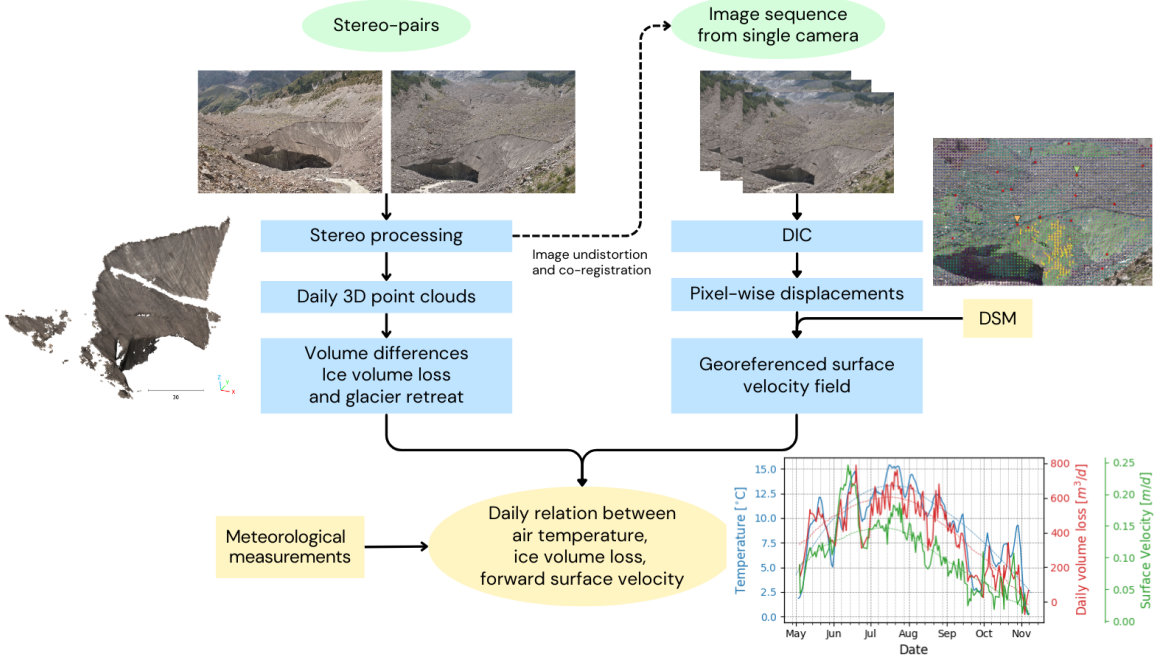


Figure 4.8: General workflow with two parallel processing chains involving stereoscopic reconstruction of terminal ice cliff from stereo-pairs of images to derive ice volume losses at the glacier terminus and glacier retreat and monoscopic digital-image correlation to derive surface velocities.

the following objectives: (i) selecting only one image per day; (ii) rejecting poor quality images that were not automatically rejected, and images in which the fixed targets placed along the moraines were not visible; (iii) detecting of sudden changes in the morphology of the glacier terminus (e.g., icefall).

4.4.2 CAMERA CALIBRATION

Each camera was mounted with all its electronics inside a waterproof case and protected by a neutral filter that was glued to the case and fixed in front of the cameras. Since the filter introduced additional distortion, the cameras need to be calibrated inside the boxes to reproduce the final setup. Therefore, a two-step approach was taken: first, a 120 cm x 70 cm calibration board with a checkerboard printed on it was used to estimate an initial set of parameters for the interior orientation (?). To this end, the cameras were mounted on tripods inside their cases while the calibration board was moved and rotated in front of the camera to simulate a convergent hemispheric acquisition. For each camera, about 30 images were collected and processed in Agisoft Metashape to obtain a first estimate of the interior orientation. However, the average camera-to-panel distance was much smaller than the actual camera-to-glacier distance. Therefore, a refinement of the calibration was performed

in-situ by incorporating the stereo pair acquired by the cameras on 28/07/22, within the UAV-A block, carried out on the same day. This block was processed with Agisoft Metashape to refine the interior camera orientation of the stereo cameras, aided by the increased robustness of the block given by the additional matches between the two images taken by camera C₁ and C₂ and the UAV.

An additional challenge was represented by camera interior orientation stability over time. From experimental evidence, the interior orientation parameter that suffered the most because of temperature variations that occurred in mountain environment was the camera principal distance (?), while the other parameters remained more stable during time. To mitigate the impact of temperature-induced variations, it was crucial to incorporate camera self-calibration during the stereoscopic processing at each epoch to refine the pre-calibrated principal distance.

4.4.3 CAMERA STABILITY AND GCPs

Since the two cameras were mounted on topographic tripods, the stability of the cameras was not perfectly guaranteed. In particular, the two cameras experienced small vibrations around their pivots due to wind gusts. On the other hand, the position of the cameras was constrained by topographic heads that kept the position of the camera center constant to the centimeter level. Therefore, the baseline of the cameras can be reasonably considered as constant, with a value of 261.55 m. On the other hand, camera angular vibrations implied that the relative orientation of the cameras must be estimated at each epoch. Moreover, to fix the world reference system over time, absolute orientation of the stereo model was required. To this end, the position of the cameras was measured in-situ using a topography-grade GNSS receiver in RTK. In addition, four GCPs were materialized with plastic targets, anchored to stable rocks in front of the terminal ice cliff and along the streamwise left moraine (Fig. ??a). While the minimum requirement to estimate a Helmert transformation would have been just the two cameras' location and one GCP, having a redundant number of GCPs overcomes the possibility that on some days not all GCPs were clearly visible in the images due to low clouds or fog. Additionally, GCPs can be included into the BA to refine the cameras' interior orientation, and in particular the camera's focal length.

As the cameras are subjected to slight rotations, the image coordinates of the GCPs' projections must be detected at each epoch. To this end, a feature tracking routine was developed based on the ImGRAFT TemplateMatch method (?), enabling the detection of a template defined on a reference image within a target image through DIC. The routine utilized the orientation correlation algorithm (?), providing increased robustness against illumination changes and achieving sub-pixel accuracy (??).

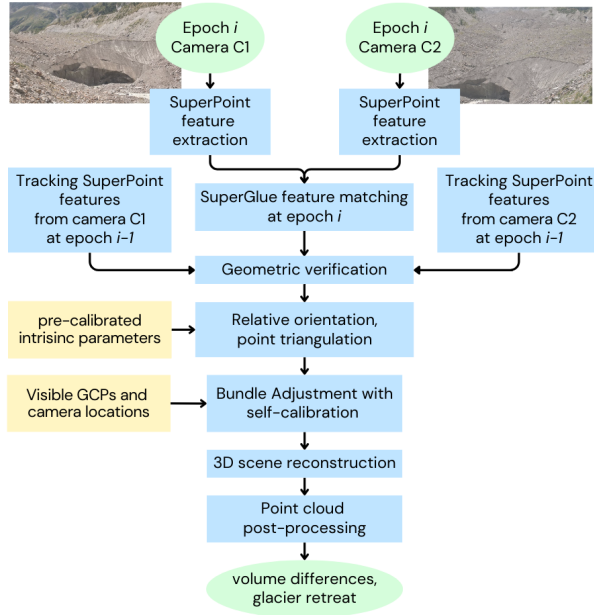


Figure 4.9: Scheme of the stereoscopic workflow performed with ICEPy4D. At a generic epoch i , new features are extracted and matched. At the same time, features from the previous epoch $i - 1$ are tracked on the current epoch images. After geometric verification, features successfully matched are used for 3D scene reconstruction. Point clouds obtained on different days are used to compute ice volume differences and glacier retreat.

4.4.4 STEREOSCOPIC IMAGE PROCESSING WORKFLOW

5

Results

LOREM IPSUM DOLOR SIT AMET, consectetur adipiscing elit. Morbi commodo, ipsum sed pharetra gravida, orci magna rhoncus neque, id pulvinar odio lorem non turpis. Nullam sit amet enim. Suspendisse id velit vitae ligula volutpat condimentum. Aliquam erat volutpat. Sed quis velit. Nulla facilisi. Nulla libero. Vivamus pharetra posuere sapien. Nam consectetur. Sed aliquam, nunc eget euismod ullamcorper, lectus nunc ullamcorper orci, fermentum bibendum enim nibh eget ipsum. Donec porttitor ligula eu dolor. Maecenas vitae nulla consequat libero cursus venenatis. Nam magna enim, accumsan eu, blandit sed, blandit a, eros.

6

Discussion

LOREM IPSUM DOLOR SIT AMET, consectetur adipiscing elit. Morbi commodo, ipsum sed pharetra gravida, orci magna rhoncus neque, id pulvinar odio lorem non turpis. Nullam sit amet enim. Suspendisse id velit vitae ligula volutpat condimentum. Aliquam erat volutpat. Sed quis velit. Nulla facilisi. Nulla libero. Vivamus pharetra posuere sapien. Nam consectetur. Sed aliquam, nunc eget euismod ullamcorper, lectus nunc ullamcorper orci, fermentum bibendum enim nibh eget ipsum. Donec porttitor ligula eu dolor. Maecenas vitae nulla consequat libero cursus venenatis. Nam magna enim, accumsan eu, blandit sed, blandit a, eros.

7

Conclusion

Lorem ipsum dolor sit amet, consectetuer adipiscing elit. Morbi commodo, ipsum sed pharetra gravida, orci magna rhoncus neque, id pulvinar odio lorem non turpis. Nullam sit amet enim. Suspendisse id velit vitae ligula volutpat condimentum. Aliquam erat volutpat. Sed quis velit. Nulla facilisi. Nulla libero. Vivamus pharetra posuere sapien. Nam consectetuer. Sed aliquam, nunc eget euismod ullamcorper, lectus nunc ullamcorper orci, fermentum bibendum enim nibh eget ipsum. Donec porttitor ligula eu dolor. Maecenas vitae nulla consequat libero cursus venenatis. Nam magna enim, accumsan eu, blandit sed, blandit a, eros.

A
A

Lorem ipsum dolor sit amet, consectetur adipiscing elit. Morbi commodo, ipsum sed pharetra gravida, orci magna rhoncus neque, id pulvinar odio lorem non turpis. Nullam sit amet enim. Suspendisse id velit vitae ligula volutpat condimentum. Aliquam erat volutpat. Sed quis velit. Nulla facilisi. Nulla libero. Vivamus pharetra posuere sapien. Nam consectetur. Sed aliquam, nunc eget euismod ullamcorper, lectus nunc ullamcorper orci, fermentum bibendum enim nibh eget ipsum. Donec porttitor ligula eu dolor. Maecenas vitae nulla consequat libero cursus venenatis. Nam magna enim, accumsan eu, blandit sed, blandit a, eros.

References

- agisoftAgisoft. 2023. Metashape. Metashape. <https://www.agisoft.com>
- Dematteis2021Dematteis, N. Giordan, D. 2021. Comparison of Digital Image Correlation Methods and the Impact of Noise in Geoscience Applications Comparison of digital image correlation methods and the impact of noise in geoscience applications. *Remote Sensing* 13, 2. 10.3390/rs13020327
- Diolaiuti2003Diolaiuti, G., D'Agata, C. Smiraglia, C. 2003. Belvedere Glacier, Monte Rosa, Italian Alps: Tongue Thickness and Volume Variations in the Second Half of the 20th Century Belvedere Glacier, Monte Rosa, Italian Alps: Tongue Thickness and Volume Variations in the Second Half of the 20th Century. *Arctic, Antarctic, and Alpine Research* 35, 2, 255–263. 10.1657/1523-0430(2003)035[0255:BGMRIA]2.0.CO;2
- Elias2020Elias, M., Eltner, A., Liebold, F. Maas, HG. 2020. Assessing the Influence of Temperature Changes on the Geometric Stability of Smartphone- and Raspberry Pi Cameras Assessing the influence of temperature changes on the geometric stability of smartphone- and raspberry pi cameras. *Sensors* 20, 3. 10.3390/s20030643
- emnifyEmnify. 2023. <https://www.emnify.com/>. [Online; visited on 22/2/2023]
- pvgisEU Science Hub - Photovoltaic Geographical Information System (PVGIS). EU Science Hub - Photovoltaic Geographical Information System (PVGIS). 2023. https://re.jrc.ec.europa.eu/pvg_tools/en/ [Online; visited on 15/11/2023]
- fitch2002OFitch, A., Kadyrov, A., Christmas, WJ. Kittler, J. 2002. OrientationCorrelation. *Orientationcorrelation.BMVCBm-10*.
- Haeberli2002Haeberli, W., Kääb, A., Paul, F., Chiarle, M., Mortara, G., Mazza, A. Richardson, S. 2002. A surge-type movement at Ghiacciaio del Belvedere and a developing slope instability in the east face of Monte Rosa, Macugnaga, Italian Alps A surge-type movement at Ghiacciaio del Belvedere and a developing slope instability in the east face of Monte Rosa, Macugnaga, Italian Alps. *Norsk Geografisk Tidsskrift* 62, 104–111. 10.1080/002919502760056422
- Heid2012e_xvaluation_{corr}Heid, T. Kb, A. 2012. Evaluation of existing image matching methods for deriving glacier surface displacement
- ioli2023,replicableIoli, F., Bruno, E., Calzolari, D., Galbiati, M., Mannocchi, A., Manzoni, P. Pinto, L. 2023. A Replicable Open

Kaab2004Kääb, A., Huggel, C., Barbero, S., Chiarle, M., Cordola, M., Epifani, F. Haeberli, W. 2004. Glacier Hazards At Belvedere Glacier and the Monte Rosa East Face , Italian Alps: Processes and Mitigation Glacier Hazards At Belvedere Glacier and the Monte Rosa East Face , Italian Alps: Processes and Mitigation. Internationales Symposion INTERPRAEVENT 2004 – RIVA / TRIENTVc67–78.

Kaab2005Kääb, A., Huggel, C., Fischer, L., Guex, S., Paul, F., Roer, I. Weidmann, Y. 2005. Remote sensing of glacier-and permafrost-related hazards in high mountains: an overview. *Remote sensing of glacier-and permafrost-related hazards in high mountains: an overview.* Natural Hazards and Earth System Sciences 5:527–554.

Messerli2015Messerli, A. Grinsted, A. 2015. Image georectification and feature tracking toolbox: ImGRAFT. *Image georectification and feature tracking toolbox: ImGRAFT.* Geoscientific Instrumentation, Methods and Data Systems 4:123–34. 10.5194/gi-4-23-2015

Mortara2009Mortara, G., Tamburini, A., Ercole, G., Semino, P., Chiarle, M., Godone, F. Valsesia, T. 2009. Il ghiacciaio del Belvedere e l'emergenza del Lago Effimero. Regione Piemonte Il ghiacciaio del belvedere e l'emergenza del lago effimero. regione piemonte. Societa' Meteorologica Subalpina.

Roethlisberger1985Roethlisberger, H., Haeberli, W., Schmid, W., Biolzi, M. Pika, J. 1985. Studi Sul Comportamento Del Ghiacciaio Del Belvedere Studi Sul Comportamento Del Ghiacciaio Del Belvedere. Comunità montana della Valle Anzasca 97.3.

greigSheridan, G. 2021. Intervalometerator Version 4.4.3. Intervalometerator Version 4.4.3. <https://github.com/greiginsydney/Intervalometerator>.

tsai2008entropyTsai, D.Y., Lee, Y., Matsuyama, E. 2008. Information entropy measure for evaluation of image quality. *Information entropy measure for evaluation of image quality.* Journal of Digital Imaging 21:338–347. 10.1007/s10278-007-9044-5

Yao_021Yao, G., Yilmaz, A., Meng, F., Zhang, L. 202101. *Review of Wide – Baseline Stereo Image Matching Based on Deep Learning*

zhangflexible_000Zhang, Z. 2000. *A flexible new technique for camera calibration*. *A flexible new technique for camera calibration.* IEEE